Catalytic Degradation and Adsorption of Metaldehyde from Drinking Water by Functionalized Mesoporous Silicas and Ion-Exchange Resin

Bing Tao and Ashleigh J. Fletcher*

Chemical and Process Engineering, Faculty of Engineering, University of Strathclyde, Glasgow, UK, G1 1XW

* Corresponding author: e-mail: ashleigh.fletcher@strath.ac.uk; tel: +44(0)141 5482431

Abstract

Sulfonic acid functionalized mesoporous silicas with various loadings of acid functionality were synthesized, characterized and applied as heterogeneous catalysts for the degradation of metaldehyde, a persistent organic pollutant in water supplies. Nuclear magnetic resonance spectroscopy showed that acetaldehyde was the only by-product of catalytic degradation, and a detailed mechanism is proposed. Kinetic studies revealed that catalyst performance is related to the accessibility of metaldehyde to active sites, such that high sulfonic acid content is undesirable since it reduces pore size, and decreases pore volume and surface area. Acetaldehyde produced via catalytic degradation, was successfully removed via chemisorption on a second mesoporous silica adsorbent modified with amine functionalities. However, limited by the surface condensation reaction mechanism, mesoporous adsorbents are less desirable than macroporous materials, with respect to acetaldehyde removal, hence, a macroporous ion-exchange resin was employed, which showed much superior performance than the amine modified silica, with a maximum capacity up to 441 mg/g. A dual-stage method is proposed to completely remove metaldehyde from drinking water by initial degradation of metaldehyde, using sulfonic acid functionalized mesoporous silica, into a single by-product, acetaldehyde, removed via chemisorption on amine bearing macroporous ion-exchange resin. The results present a promising system for removal of metaldehyde from drinking water supplies, with potential application to other contaminants.

Keywords: Heterogeneous catalysis; Dual-stage column; Acetaldehyde; Sulfonic Acid; Amines; GC-FID; HPLC.

1. Introduction

Metaldehyde contamination of drinking water has attracted extensive attention since it was highlighted by the UK environmental agency in 2008 [1]. As a molluscicide, metaldehyde is used widely by farmers and gardeners to protect crops and garden vegetation from slugs and snails; however, quantities are washed off the land into streams and rivers, subsequently entering drinking water supplies where existing treatment methods fail to remove it to the current UK/EU standards of 0.1 μg L^{-1} [2]. In recent years, steps have been taken to combat this issue, however, these initiatives have not produced the results expected and, according to the latest British Geological survey and Water UK briefing, metaldehyde concentrations in many areas still exceed European and UK drinking water standards [3], with several regions reporting amounts higher than 10 times than permitted levels [4]. Concurrently, fundamental research has seen extensive work to control the situation but proposed methods are either prohibitively expensive [5] or suffer by-product issues [5, 6].

Highly ordered mesoporous silicas, first synthesized in 1998 [7], especially materials incorporating different organic functional groups, have been explored for applications such as ion exchange [8], heavy-metal-trapping [9, 10] and solid acid catalysis [11, 12]. In the case of solid acid catalysts, sulfonic acid functionalized SBA-15 has been extensively synthesized and used in esterification reactions [13-15]. The highly ordered uniform structure, high sure face area and big pore volume [16] have also allowed mesoporous silicas to be applied as adsorbents and it has been reported that mesoporous SBA-15 is an effective adsorbent for the remediation of selected pharmaceuticals from surface water and wastewater, through the mechanism of hydrophilic reactions [16]. Moreover, mesoporous silica has been applied for removal of various organics such as phenolic compounds [17, 18], and cyanuric acid [18]. Here we report the synthesis, characterization and application of

sulfonic acid functionalized SBA-15 materials as effective catalysts for the depolymerisation of metaldehyde into acetaldehyde, and subsequent optimization of the chemisorption of this single by-product to achieve the ultimate goal of complete removal of metaldehyde from drinking water.

2. Experimental

2.1 Materials used

The synthesis of sulfonic acid functionalized mesoporous silicas (SA-SBA-15) was similar to that described previously [13, 15, 19]. Typically, 4 g of pluronic acid 123 (Aldrich) was dissolved in 125 g of 1.9 M HCl and the resulting solution heated to 313 K before addition of tetraethoxysilane (TEOS), 3-mercaptopropyltrimethoxysilane (MPTMS) and 30 wt% H_2O_2 solution, all supplied by Sigma-Aldrich Co. The molar composition of the different mixtures for 4 g of copolymer was set as TEOS/MPTMS = 0.041(1-x)/0.041x, where x = 0.1, 0.2, 0.33, 0.5, 0.75, corresponding to functionalization levels of 10, 20, 33, 50 and 75%. The molar amount of H_2O_2 was kept at 10 times that of MPTMS. The mixture was stirred at 313 K for 20 h, aged at 373 K for 24 h, then filtered and dried at room temperature overnight. Dried samples were extracted using absolute ethanol under reflux to remove the template. Amine functionalized silicas (AF-SBA-15) were synthesized using a similar procedure, with TEOS and 3-aminopropyltrimethoxysilane, as described previously [19]. Macroporous ion exchange resin A830 was supplied by Purolite, UK; the sample incorporates a number of complex amine functional groups.

2.2 Experimental techniques

As-prepared silica samples were characterized by small-angle powder X-ray diffraction (PXRD), using X'pert pro, from Panalytical, to determine structural characteristics. Textural characterization was performed using nitrogen sorption measurements on an ASAP 2420 supplied by Micrometrics, at 77 K. Surface areas were calculated using the Brunauer-Emmet-Teller (BET) method [20]. Pore size distributions were calculated using the Barrett-

Joyner-Halenda (BJH) model applied to the desorption isotherm branch [21]. Scanning electron microscopy (SEM) was carried out on a Hitachi S-3700N system. Sulfonic acid contents (SAC) of SA-SBA-15 were determined by titration, as described elsewhere [13, 15]. Nitrogen contents of AF- SBA-15 were determined by CHN elemental analysis. Nuclear Magnetic Resonance (NMR) spectra were recorded on a Bruker AV400 system.

Heterogeneous catalytic degradation of metaldehyde using SA-SBA-15, with varied SA loadings, was performed by adding 200 mg of catalyst to 200 mL of metaldehyde solution with initial concentration 200 mg g^{-1} (5.6812 mmol L^{-1}). Samples were taken at predetermined time intervals and the concentration of metaldehyde and acetaldehyde determined. The kinetic investigation of acetaldehyde chemisorption onto AF-SBA-15 and A830was performed by adding 100 mg of adsorbent to 200 mL acetaldehyde solution with initial concentration of 20 mg L^{-1}. Samples were taken at selected time intervals. The adsorption isotherm of acetaldehyde onto A830 at 293 K was determined by bottle-point method, where 50 mg of A830 was added to 200 mL of acetaldehyde solutions with varying concentrations and the system allowed to equilibrate.

Metaldehyde concentrations of aqueous samples were determined by gas chromatography (GC), as described previously [2]. Acetaldehyde concentrations were determined using a Shimadzu Prominence high performance liquid chromatograph (HPLC) equipped with UV-Vis detector. Water samples were reacted with 2,4-dinitrophenyhydrazine (DNPH), 97% purity supplied by Sigma-Aldrich Co., to yield acetaldehyde-DNPH, which was detected by UV-Vis. A VP-ODS column (150 mm L × 4.6 mm D), supplied by Shimadzu, was used for separation and the mobile phase was 50/50 v/v water/acetonitrile, with a flow rate 1.5 mL min^{-1}. The wavelength was set as 365 nm. An external standard quantification method was applied and analytical standard grade acetaldehyde-DNPH, supplied by Supelco, used as the external standard material.

3. Results and discussion

3.1 Materials characterization

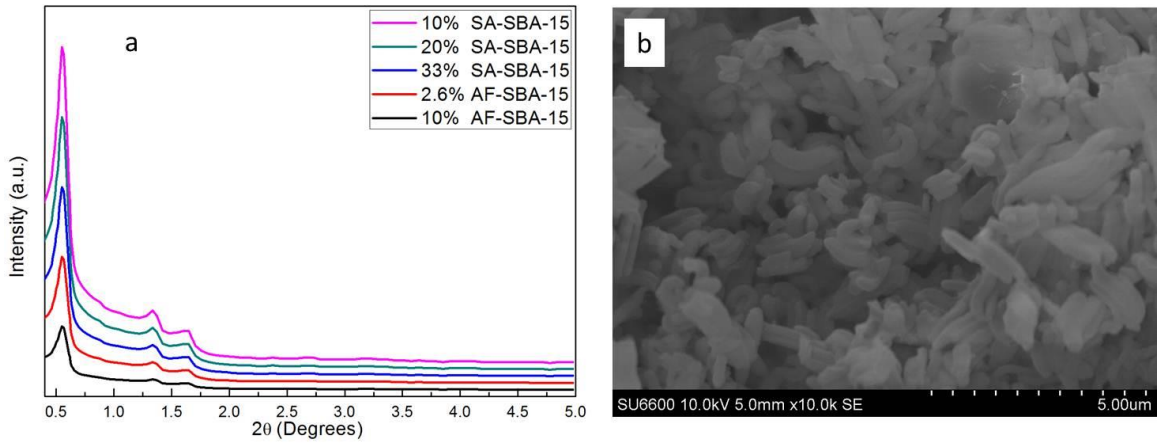

Figure 1: a) low-angle PXRD patterns of as-synthesized sulfonic acid and AF-SBA-15; b) scanning electron micrograph of as-synthesized 10% SA-SBA-15 with magnification 10,000x.

Figure 1a shows the small-angle PXRD pattern of five functionalized silica samples synthesized in this study. Three of the five SA-SBA-15 samples, i.e. those at 10%, 20% and 33%, exhibited three well-resolved peaks, which can be indexed as (1 0 0), (1 1 0) and (2 0 0); these are known diffractions associated with the highly ordered two-dimensional hexagonal symmetry (space group p6mm) of mesoporous silica SBA-15. Although it has been reported that functionalization could go as high as 60% [22, 23], in this work silicas with SAC > 75% failed to form solids, and samples with SAC of 50% and 75% formed solids but failed to show well-resolved PXRD peaks. Both AF-SBA-15 samples exhibited well resolved peaks, indicating highly ordered mesoporous structures for these samples. SEM images, shown in Figure 1b, reveal that the as-prepared silica samples consist of many rope-like domains with relatively uniform sizes, aggregated into wheat-like macrostructures similar to those found for conventional unmodified SBA-15 [7, 15].

Figure 2 shows nitrogen sorption isotherms and pore size distributions for all SA-SBA-15 samples, and it is evident that three well-distinguished regions of the isotherms can be identified, indicating some small micropore capacity, capillary condensation, showing the presence of mesopores, and eventual plateauing at high relative pressures. Titration results,

calculated structural parameters, BET surface areas and pore volumes are given in Table 1. Pore volumes were determined from the $p/p_0 = 0.985$ adsorption point ,and pore sizes were calculated using BJH analysis [21].

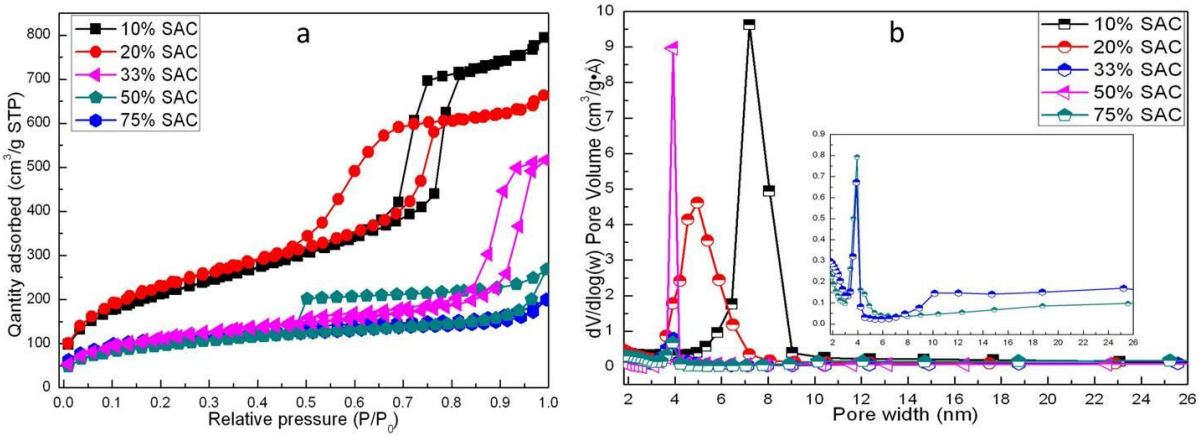

Figure 2: a) nitrogen sorption isotherms at 77 K for as-synthesized SA-SBA-15 with different sulfonic acid contents (SAC); b) pore size distributions for as-synthesized SA-SBA-15 samples.

It is clear, from Figure 2b, that significant shrinkage in mesopore diameter is observed as SAC increases. Also, broader hysteresis loops were observed for samples with higher SAC, as seen in Figure 2a, again indicating partial blockage of the pores. Partial pore blockage in SBA-15 by organic functional groups has been observed extensively [22, 24-27], and is notable at pore entrances [23], and the observation of a H2 hysteresis loop in highly functionalized samples confirms the presence of blocking effects [28]. The observed decrease in pore volumes and surface areas for high SAC materials, shown in Table 1, is also ascribed to pore blocking.

Table 1: Textural parameters, titration results and first order rate constants for as-synthesized sulfonic acid functionalized silica samples

Level of acid functionalization	S_{BET} ($m^2\ g^{-1}$)	APD (nm)	PV ($cm^3\ g^{-1}$)	SAC (mmol g^{-1})	k (min^{-1})
10%	828 ± 6.5	7.16	1.23	1.28	3.2×10^{-3}
20%	770 ± 4.5	5.06	1.03	1.71	2.4×10^{-3}
33%	350 ± 6.8	3.95	0.31	1.94	1.5×10^{-4}
50%	334 ± 3.8	3.81	0.41	2.05	1.3×10^{-4}
75%	394 ± 3.5	3.79	0.79	2.09	1.2×10^{-4}

APD = Average Pore Diameter; PV = Pore Volume; SAC = Sulfonic Acid Content; k = first-order rate constant.

3.2 Catalytic degradation of metaldehyde

It is has been reported that metaldehyde can be degraded by the presence of strong acids (e.g. HCl) [29, 30], but no detailed mechanism has yet been presented. Since $-SO_3H$ has very similar properties to HCl, it is reasonable to propose that $-SO_3H$ can similarly catalyze the depolymerisation reaction of metaldehyde, and a detailed mechanism, for sulfonic functionalities tethered to silica, is proposed in Figure 3.

It has also been reported that ether functionalities can be cleaved by strong acids [31], and, initially, the authors assumed that the removal mechanism would be based on cleavage of the ether bond by sulfonic acid functionalities [2]. However, the experimental work undertaken herein, using a continuous fixed bed column reactor, has indicated that a by-product exists in the effluent, which was masked in previous 'batch' studies [2] as a result of the contact times used and the position of the solvent peak; an additional peak was detected in the gas chromatograph, corresponding to acetaldehyde. Furthermore, NMR spectra, of which representative examples are shown in Figure 4, revealed that after treatment with 10% SA-SBA-15 the peaks corresponding to metaldehyde (d at 1.4, q at 5.4ppm) decreased to almost negligible levels as reaction time elapsed, with only characteristic peaks for

acetaldehyde (d at 2.2, s at 9.6ppm), and no other intermediates or by-products, observed. Full NMR data are available in Supporting Information.

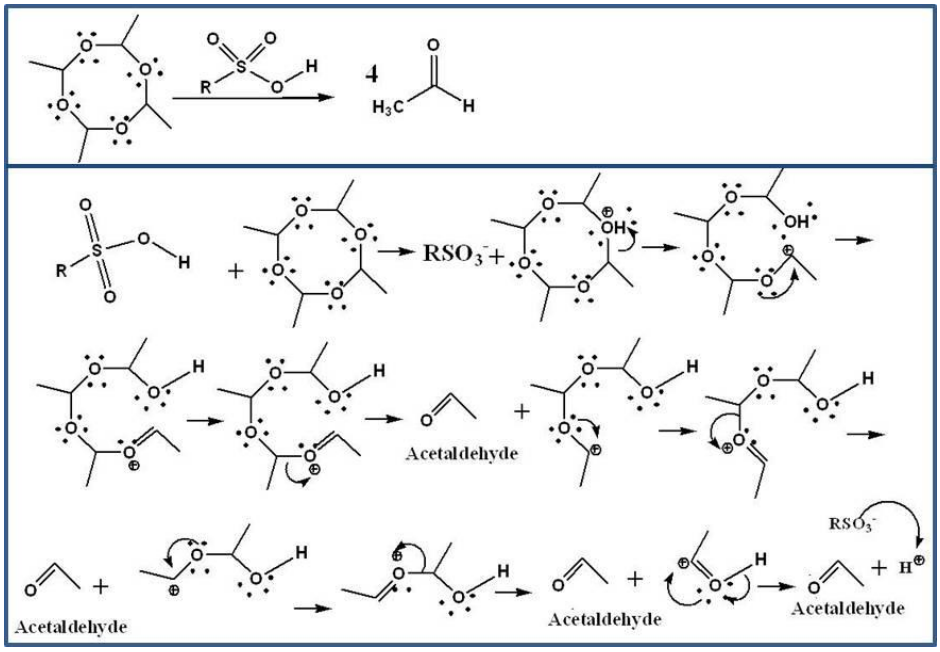

Figure 3: mechanism for depolymerisation of metaldehyde by sulfonic acid functionalized SBA-15

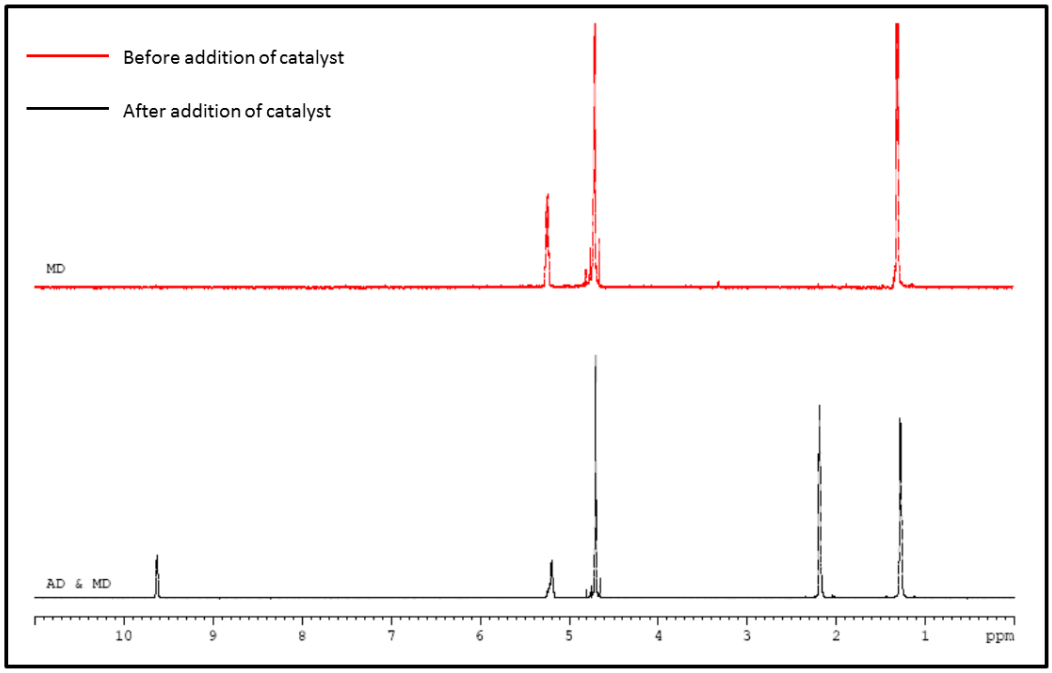

Figure 4: NMR spectra of metaldehyde (in D_2O) before and after addition of 10% SA-SBA-15.

As a consequence of the improved understanding of the underlying mechanism, it was possible to determine the efficiency of the process. Catalytic activity is a significant

parameter that measures the efficiency of a catalyst in converting reactants to products; the activity of a catalyst is defined as the rate of consumption of reactant, hence, the kinetics of the catalytic reactions were investigated, using:

$$\text{Metaldehyde (MD, } C_8H_{16}O_4,) \xrightarrow{\text{Catalyst (C, } RSO_3H)} \text{Acetaldhyde (AD, } C_2H_4O)$$

$$r = -\frac{d[MD]}{dt} = k_{MD,C} \times [MD] \times [C] = k'_{MD} \times [MD] \quad (1)$$

where r is the reaction rate of metaldehyde, [ ] denotes molar concentrations, $k_{MD,C}$ represents the second-order rate constant ($mol^{-1}\ s^{-1}$) and k'_{MD} is the first-order rate constant (s^{-1}). Since the concentration of the catalyst is constant, and in significant excess, the rate of reaction is only dependent on the concentration of metaldehyde; therefore, a first-order rate Equation can be employed:

$$\frac{C_t}{C_0} = e^{-k'_{MD}t} \quad (2)$$

where C_t is the concentration at time t, and C_0 is initial concentration. Figure 5a shows the concentration evolution of metaldehyde as a function of time for silica samples with increasing SAC, and the resulting fits to the first-order kinetic equation; the rate constants, k, obtained are shown in Table 1. It is clear that the rate of reaction decreases with increasing SAC, and 10% SA-SBA-15 showed the best kinetic performance, with a rate constant one order of magnitude higher than all other samples studied. It may be expected that increasing quantities of active acid groups would enhance the rate of degradation but, as stated earlier, high SAC reduces the surface area, pore size and pore volume, such that the most important step of the catalytic reaction, reactant diffusion from the bulk solution to reactive catalyst sites, is hindered by increasing diffusive resistance, reducing the reaction rate. Furthermore, the blocking of well-ordered pores by organic functional groups, especially significant blockage at pore entrances, also impedes the access of metaldehyde molecules to reactive sites. Figure 5b displays changes in molar concentration for metaldehyde and acetaldehyde as a function of time, using 10% SA-SBA-15 as catalyst. It is expected from

Equation (1) that the maximum theoretical change in molar acetaldehyde concentration should be 4 times that of the decrease in metaldehyde concentration, due to the production of 4 acetaldehyde molecules per each metaldehyde molecule degraded. It is clearly shown, in Figure 5b, that the experimental data fits the theoretical data extremely well, confirming the proposed mechanism quantitatively.

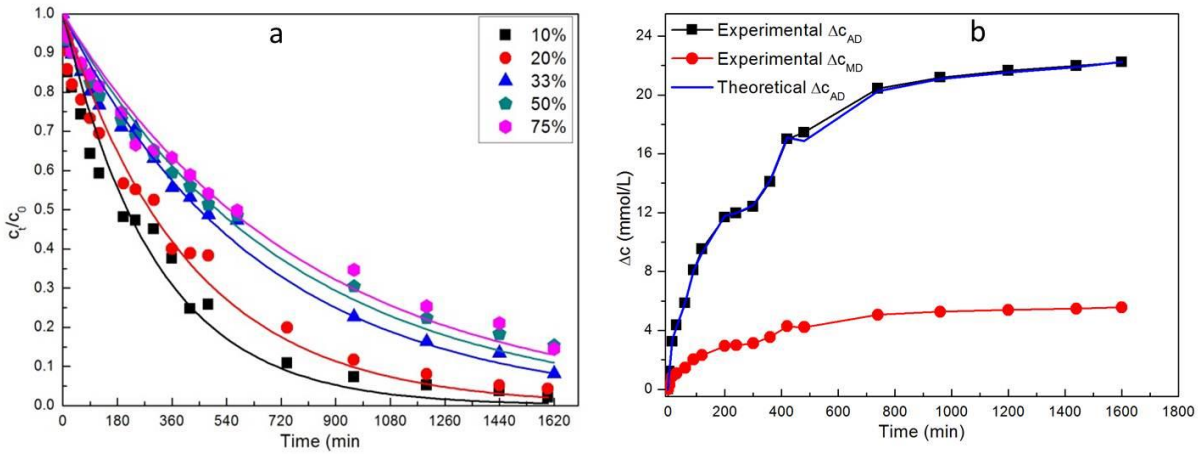

Figure 5: a) kinetics of metaldehyde depolymerisation using as-synthesized SA-SBA-15 samples; b) change in molar concentration of metaldehyde and acetaldehyde as a function of time using 10% SA-SBA-15 as catalyst; $\Delta c_{AD} = c_{t,AD}$, $\Delta c_{MD} = c_{0,MD} - c_{t,MD}$

3.3 Acetaldehyde adsorption

It has been reported that vapor phase acetaldehyde can be adsorbed by amine functionalized materials via the following condensation reaction [32, 33]:

$$H_2N - R + CH_3CHO \rightarrow CH_3CH = N - R + H_2O \quad (3)$$

It was assumed, by the authors, that a similar reaction would be possible in the aqueous phase, hence, in order to remove the single by-product of the catalytic degradation of metaldehyde, materials with amine functionality were applied to treated aqueous phase samples. As stated earlier, SBA-15 has a tunable, highly ordered, uniform structure, high sure face area, large pore volume and, most importantly, the ability to host various organic functionalities. Hence, it was possible to synthesize SBA-15 with amine functionalities (AF-SBA-15), which was applied for the removal of acetaldehyde. The amine content was kept low at only 2.6% and 10% as a result of the expected pore blocking effect for higher

concentrations, as observed for SA-SBA-15. Small-angle powder XRD patterns of the AF-SBA-15 samples exhibited similar characteristic peaks to SA-SBA-15 (Figure 1a). Nitrogen adsorption characterization results of these two samples are shown in Table 3, as well as the nitrogen contents determined by CHN analysis. It can be clearly seen from Table 3 that the inclusion of amine functionalities partially reduced the silica porosity, causing a decrease in surface area from 420 $m^2 g^{-1}$ (2.6%) to 291 $m^2 g^{-1}$ (10%). A similar trend in pore volume was observed for pore volume, with a decrease from 0.41 $cm^3 g^{-1}$ to 0.23 $cm^3 g^{-1}$ as amine content increased.

Table 2: Textural parameters, nitrogen contents and pseudo-second order rate constants for as-synthesized AF-SBA-15 and ion exchange resin A830

Sample code	S_{BET} ($m^2 g^{-1}$)	APD (nm)	PV ($cm^3 g^{-1}$)	NC (%)	k_2 (min^{-1})
AF-SBA-15 2.6%	420 ± 1.1	3.5	0.41	0.23	5.37×10^{-3}
AF-SBA-15 10%	291 ± 1.9	3.4	0.23	1.39	1.33×10^{-2}
A830	1.82 ± 0.06	>100	0.01	2.14	3.04×10^{-3}

APD = Average Pore Diameter; PV = Pore Volume; NC = Nitrogen Content, determined by elemental analysis; k_2 = pseudo-second-order rate constant[2].

As-synthesized AF-SBA-15 were applied to remove acetaldehyde from prepared samples and Figure 6a shows the kinetic profiles of sorption at 293 K. The experimental data were fitted to pseudo-first order and pseudo-second kinetic equations [2], And the modeling showed that the pseudo-second order equation describes the kinetic process better than the pseudo-first order equation, with the pseudo-second order rate constants presented in Table 3, showing that the sorption rate of 10% AF-SBA-15 was significantly faster than that of 2.6% AF-SBA-15. However, the adsorption capacities showed the opposite trend, i.e. 2.6% AF-SBA-15 demonstrated a greater capacity than that of 10% AF-SBA-15. These contradictory results are closely related to the pore structure of the samples and the adsorption mechanism. Increasing amine content increases the density of active sites, enabling 10%

AF-SBA-15 a higher efficiency for capturing acetaldehyde, hence, this sample showed better kinetic performance. However, as stated above, the pore size and pore volume of 10% AF-SBA-15 were already reduced comparative to 2.6% AF-SBA-15, and as adsorption progressed, the pores became blocked further by the products of the condensation reaction, as illustrated in Equation (3). This significantly increases blocking effects in the sample with greater functionalization, which eventually hinders access of acetaldehyde molecules to the reactive sites. So, even though 10% AF-SBA-15 has a greater number of reactive sites overall, only those sites at the pore entrance are accessible, resulting in a faster kinetic performance yet lower adsorption capacity than 2.6% AF-SBA-15.

It is notable that both AF-SBA-15 samples showed low adsorption capacities an impractical aspect for use in the water treatment industry. As the results obtained for these samples suggested lack of accessibility to reactive sites is limiting to the adsorption capacity, it is reasonable to propose that materials with larger pores, such as macroporous resins may exhibit an increased capacity, where reactive site number is still significant. To test this hypothesis, a macroporous ion exchange resin (A830) with an acrylic matrix and complex amine functionalities was applied for the removal of acetaldehyde. Data for the kinetics of acetaldehyde sorption onto A830 are displayed in Figure 6a, together with comparative data for AF-SBA-15 samples. Figure 6b clearly shows that the capacity of A830 is much greater than the as-prepared mesoporous silicas; although the rate constant was much reduced, which is possibly due to the very small surface area and pore volume of the resin. Figure 6b shows the isotherm for acetaldehyde adsorption on A830 at 293 K and the subsequent fit to the Langmuir equation. The maximum capacity of A830 was obtained at 441 mg g^{-1}, indicating that materials with similar properties to A830 could be promising candidates for acetaldehyde removal. Hence, it is proposed that a novel two-staged method consisting of an initial step to degrade metaldehyde into acetaldehyde, and a second stage to adsorb the acetaldehyde formed could be developed and operated subject to further optimization.

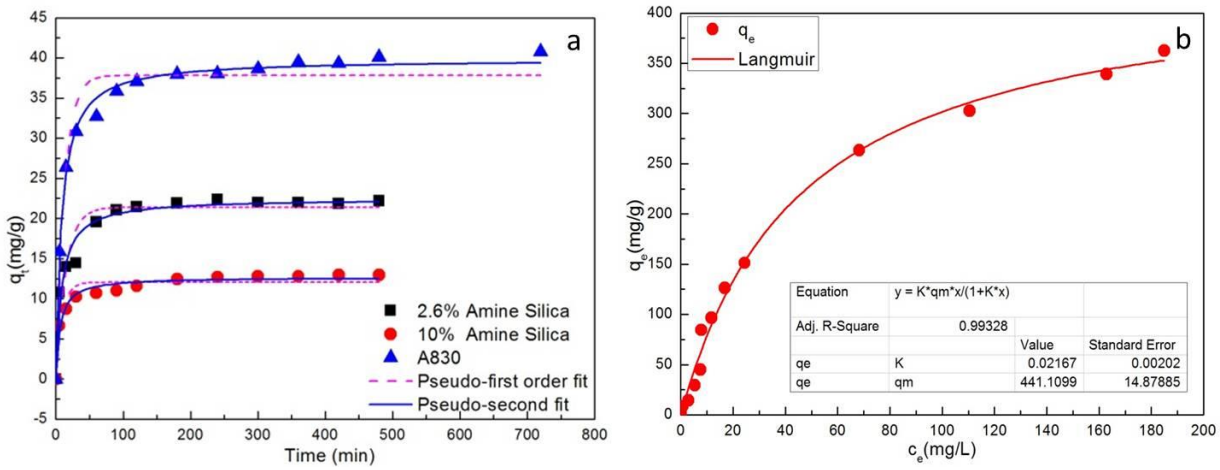

Figure 6: a) adsorption kinetics of acetaldehyde onto AF-SBA-15 and A830 and the fitting of experimental data to different adsorption kinetic equations; b) isotherm of acetaldehyde sorption onto A830 at 293 K and the fitting to Langmuir equation.

4. Conclusions

Well-ordered mesoporous sulfonic acid and amine functionalized SBA-15 has been synthesized via triblock copolymer template reactions. Sulfonic acid functionalized SBA-15 showed excellent catalytic performance for the degradation of metaldehyde, with acetaldehyde as the only by-product. Kinetic studies showed that the rate of degradation is related to accessibility of metaldehyde molecules to the active sites present within the pores of the catalyst, such that pore size and pore volume have a dramatic effect on kinetic performance. Degradation of metaldehyde was shown to produce stoichiometric quantities of acetaldehyde and amine functionalized SBA-15 was shown to be capable of chemically adsorbing acetaldehyde through surface condensation reactions, akin to vapor phase studies, indicating that high amine content would increase adsorption capacity. However, increasing amine content decreased both pore size and pore volume of the as-made silica samples, such that acetaldehyde molecules cannot access to the functional sites, which is exacerbated by the fact that the product of the surface condensation reaction blocks the pore entrances further. Application of a macroporous adsorbent with high amine content (A830), to reduce the influence of pore blockage, showed an improved performance compared to the amine functionalized mesoporous silicas supporting the conclusion that

pore blocking reduces capacity and suggesting routes to materials development. The combined results of metaldehyde degradation and acetaldehyde adsorption indicate that a dual-stage column method could achieve total removal of metaldehyde from drinking water, via catalytic depolymerisation of metaldehyde into acetaldehyde and subsequent chemical adsorption.

Acknowledgements

The authors are thankful to Purolite (Wales, UK) for supplying the ion exchange resin (A830). B.T. thanks China Scholarship Council (CSC) and the University of Strathclyde for financial support.

References

[1] Environmetal Agency UK, Environment Agency position on Metaldehyde Version 2, in, UK, 2011.

[2] B. Tao, A.J. Fletcher, Metaldehyde removal from aqueous solution by adsorption and ion exchange mechanisms onto activated carbon and polymeric sorbents, Journal of Hazardous Materials, 244 (2013) 240-250.

[3] British Geological Survey, Emerging contaminants in groundwater, in, UK, 2011.

[4] J. Marshall, Water UK Briefing-Metaldehyde 2011, in, UK, 2011.

[5] O. Autin, J. Hart, P. Jarvis, J. MacAdam, S.A. Parsons, B. Jefferson, Comparison of UV/H_2O_2 and UV/TiO_2 for the degradation of metaldehyde: Kinetics and the impact of background organics, Water Res., (2012).

[6] F.C. Doria, A. Borges, J. Kim, A. Nathan, J. Joo, L. Campos, Removal of Metaldehyde Through Photocatalytic Reactions Using Nano-Sized Zinc Oxide Composites, Water Air Soil Poll., 224 (2013) 1-9.

306 [7] D. Zhao, J. Feng, Q. Huo, N. Melosh, G.H. Fredrickson, B.F. Chmelka, G.D. Stucky,
307 Triblock copolymer syntheses of mesoporous silica with periodic 50 to 300 angstrom pores,
308 Science, 279 (1998) 548-552.

309 [8] V. Ganesan, A. Walcarius, Surfactant templated sulfonic acid functionalized silica
310 microspheres as new efficient ion exchangers and electrode modifiers, Langmuir, 20 (2004)
311 3632-3640.

312 [9] X. Feng, G. Fryxell, L.-Q. Wang, A.Y. Kim, J. Liu, K. Kemner, Functionalized monolayers
313 on ordered mesoporous supports, Science, 276 (1997) 923-926.

314 [10] T. Pinnavaia, Selective adsorption of Hg2+ by thiol-functionalized nanoporous silica,
315 Chem.Commun., (1999) 69-70.

316 [11] D. Das, J.-F. Lee, S. Cheng, Sulfonic acid functionalized mesoporous MCM-41 silica as
317 a convenient catalyst for Bisphenol-A synthesis, Chem.Commun., (2001) 2178-2179.

318 [12] W. Van Rhijn, D. De Vos, B. Sels, W. Bossaert, Sulfonic acid functionalised ordered
319 mesoporous materials as catalysts for condensation and esterification reactions,
320 Chem.Commun., (1998) 317-318.

321 [13] J.G. Shen, R.G. Herman, K. Klier, Sulfonic acid-functionalized mesoporous silica:
322 Synthesis, characterization, and catalytic reaction of alcohol coupling to ethers,
323 J.Phys.Chem. B, 106 (2002) 9975-9978.

324 [14] I.K. Mbaraka, D.R. Radu, V.S.-Y. Lin, B.H. Shanks, Organosulfonic acid-functionalized
325 mesoporous silicas for the esterification of fatty acid, J. Catal., 219 (2003) 329-336.

326 [15] D. Margolese, J. Melero, S. Christiansen, B. Chmelka, G. Stucky, Direct syntheses of
327 ordered SBA-15 mesoporous silica containing sulfonic acid groups, Chem. Mater., 12 (2000)
328 2448-2459.

329 [16] T.X. Bui, H. Choi, Adsorptive removal of selected pharmaceuticals by mesoporous silica
330 SBA-15, Journal of hazardous materials, 168 (2009) 602-608.

[17] M.C. Burleigh, M.A. Markowitz, M.S. Spector, B.P. Gaber, Porous polysilsesquioxanes for the adsorption of phenols, Environmental science & technology, 36 (2002) 2515-2518.

[18] C. Cooper, R. Burch, Mesoporous materials for water treatment processes, Water Research, 33 (1999) 3689-3694.

[19] R.K. Zeidan, S.J. Hwang, M.E. Davis, Multifunctional Heterogeneous Catalysts: SBA-15-Containing Primary Amines and Sulfonic Acids, Angew. Chem. Int.Edit., 45 (2006) 6332-6335.

[20] S. Brunauer, P.H. Emmett, E. Teller, Adsorption of gases in multimolecular layers, J. Am. Chem. Soc., 60 (1938) 309-319.

[21] E.P. Barrett, L.G. Joyner, P.P. Halenda, J. Phys. Chem., 73 (1951) 373.

[22] M. Kruk, T. Asefa, M. Jaroniec, G.A. Ozin, Metamorphosis of ordered mesopores to micropores: periodic silica with unprecedented loading of pendant reactive organic groups transforms to periodic microporous silica with tailorable pore size, J.Am. Chem. So., 124 (2002) 6383-6392.

[23] C.-T. Tsai, Y.-C. Pan, C.-C. Ting, S. Vetrivel, A.S. Chiang, G.T. Fey, H.-M. Kao, A simple one-pot route to mesoporous silicas SBA-15 functionalized with exceptionally high loadings of pendant carboxylic acid groups, Chem.Commun., (2009) 5018-5020.

[24] M. Kruk, M. Jaroniec, C.H. Ko, R. Ryoo, Characterization of the porous structure of SBA-15, Chem. Mat., 12 (2000) 1961-1968.

[25] A. Vinu, V. Murugesan, M. Hartmann, Adsorption of lysozyme over mesoporous molecular sieves MCM-41 and SBA-15: influence of pH and aluminum incorporation, The Journal of Physical Chemistry B, 108 (2004) 7323-7330.

[26] F.-K. Shieh, C.-T. Hsiao, J.-W. Wu, Y.-C. Sue, Y.-L. Bao, Y.-H. Liu, L. Wan, M.-H. Hsu, J.R. Deka, H.-M. Kao, A bioconjugated design for amino acid-modified mesoporous silicas

as effective adsorbents for toxic chemicals, Journal of hazardous materials, 260 (2013) 1083-1091.

[27] Y. Mori, T.J. Pinnavaia, Optimizing organic functionality in mesostructured silica: direct assembly of mercaptopropyl groups in wormhole framework structures, Chem. Mat., 13 (2001) 2173-2178.

[28] M. Thommes, R. Köhn, M. Fröba, Sorption and pore condensation behavior of pure fluids in mesoporous MCM-48 silica, MCM-41 silica, SBA-15 silica and controlled-pore glass at temperatures above and below the bulk triple point, Applied surface science, 196 (2002) 239-249.

[29] J. Bevington, The polymerisation of aldehydes, Quart. Rev. Chem. Soc., 6 (1952) 141-156.

[30] S. Selim, J.N. Seiber, Gas chromatographic method for the analysis of metaldehyde in crop tissue, J. Agr.Food. Chem., 21 (1973) 430-433.

[31] J.M. Michael Smith, March's Advanced Organic Chemistry: Reactions, Mechanisms, And Structure 6th Edition, John Wiley & Sons, New York, 2007.

[32] A.M. Ewlad-Ahmed, M.A. Morris, S.V. Patwardhan, L.T. Gibson, Removal of Formaldehyde from Air Using Functionalized Silica Supports, Environ. Sci. Technol., 46 (2012) 13354-13360.

[33] T. Hayashi, M. Kumita, Y. Otani, Removal of acetaldehyde vapor with impregnated activated Carbons: Effects of steric structure on impregnant and acidity, Environ. Sci. Technol., 39 (2005) 5436-5441.